

Reentrant spin glass transition in $\text{LuFe}_2\text{O}_{4-\delta}$

Fan Wang, Jung-ho Kim, and Young-June Kim*

Department of Physics, University of Toronto, Toronto, Ontario M5S 1A7, Canada

G. D. Gu

*Department of Condensed Matter and Material Science,
Brookhaven National Laboratory, Upton, New York, 11973*

(Dated: October 31, 2018)

We have carried out a comprehensive investigation of magnetic properties of LuFe_2O_4 , using AC susceptibility, DC magnetization and specific heat. A magnetic phase transition around ~ 236 K was observed with DC magnetization and specific heat measurements, which is identified as a paramagnetic to ferrimagnetic transition based on the nonlinear susceptibility data. Upon further cooling below this temperature, we also observed highly relaxational magnetic behavior: the DC magnetization exhibits history and time dependence, and the real and imaginary part of the AC susceptibility shows large frequency dependence. Dynamic scaling of the AC susceptibility data suggests that this low temperature phase can be described as a reentrant spin glass phase. We also discuss magnetic field dependence of the spin glass transition and aging, memory and rejuvenation effect below the glass transition temperature around 228 K.

PACS numbers: 75.50.Lk, 75.50.Gg, 75.40.Cx, 75.40.Gb

I. INTRODUCTION

Geometrical frustration plays an important role in determining ground states and phase transitions in magnetic systems. A triangular lattice in two-dimension in particular is one of the simplest systems to study the effect of geometrical frustration. LuFe_2O_4 is a member of RFe_2O_4 family of compounds, where R can be Y, Ho, Er, Tm, Yb, and Lu.¹ These materials all have hexagonal layered structure, in which Fe ions form a triangular lattice within each bilayer.² Since the average charge valence of Fe in this compound is $+2.5$, this system is expected to exhibit charge order behavior similar to Fe_3O_4 ^{3,4} or half doped manganites.⁵ However, due to the geometrical frustration introduced by the triangular lattice, understanding charge order in this material is not straightforward.⁶ Previous electron and x-ray diffraction studies have shown that charge ordering sets in below ~ 300 K, and anomalous dielectric dispersion was observed in this temperature range.^{6,7} In particular, Ikeda and coworkers argued that the observed pyroelectric signal below charge ordering temperature indicates charge order driven ferroelectricity.⁷ This result has been drawing much attention,^{8,9} since this would be the first such observation of ferroelectricity with electronic origin. In addition, it was observed that the pyroelectric signal shows an unusual step around the spin ordering temperature, and a large magnetodielectric response under low magnetic fields was also observed in LuFe_2O_4 at room temperature,¹⁰ which prompted further interests in this compound as a possible multiferroic (or magnetic ferroelectric) material.

Although whether the magnetic and ferroelectric order parameters are coupled in LuFe_2O_4 is not clear at the moment, LuFe_2O_4 exhibits quite interesting magnetic properties, as a result of the geometrical frustration arising

from the triangular lattice. Most of earlier studies of the magnetism in RFe_2O_4 have been focused on YFe_2O_4 . Tanaka et al. first reported that Fe spins order below 220 K based on their Mössbauer experiments.¹¹ In their studies of transport properties, they also observed that there are two distinct transitions at 240 K and 225 K, and the former corresponds to Verwey-like charge ordering accompanied by magnetic ordering.¹² This was corroborated in the x-ray study of Nakagawa and coworkers, in which first order structural phase transitions were observed around these temperatures.¹³ Recently, Ikeda et al. reported that more than two transitions exist in YFe_2O_4 based on their x-ray powder diffraction studies.¹⁴ They also argued that the transition at 250 K corresponds to charge and spin ordering.

However, it was also realized that the oxygen non-stoichiometry in YFe_2O_4 can cause significant changes in its magnetic properties, while LuFe_2O_4 is believed to be free from such oxygen non-stoichiometry problems.¹⁵ In their comprehensive magnetization and neutron scattering work on LuFe_2O_4 , Iida and coworkers were able to elucidate unusual magnetic properties of this compound.¹⁶ Specifically, they found that the system does not show any long range three-dimensional magnetic order down to 4.2 K. Instead, they argued that the system at low temperatures consists of ferrimagnetic clusters of various sizes, based on their thermoremanent magnetization measurements. The ferrimagnetism in this case arises due to the mixture of $S=2$ and $S=5/2$ spins. In recent neutron scattering experiments, however, sharp magnetic Bragg peaks were observed, suggesting existence of long-range magnetic order.^{17,18} Therefore, the nature of the ground state of LFO is still not understood well.

In this paper, we report our comprehensive study of magnetic properties of LuFe_2O_4 using AC susceptibility,

DC magnetization and specific heat. We have observed two magnetic transitions: The high temperature transition occurs at $\sim 236\text{K}$, and corresponds to the previously observed ferrimagnetic transition.^{16,17} The signature of this transition is also observed in our specific heat measurements. In addition to this ferrimagnetic transition, we observe an unusual magnetic transition at a lower temperature, which shows relaxational behavior similar to that of a spin-glass phase.

This paper is organized as follows. In the next section, we will explain our sample preparation and characterization in detail. In Sec. III, our experimental results from magnetic susceptibility and specific heat measurements are presented. In Sec. IV, we will discuss the implication of the observed results, and possible connection with the charge order and ferroelectricity.

II. EXPERIMENTAL DETAILS

LuFe_2O_4 (LFO) single crystals were grown using the travelling solvent floating zone method at Brookhaven National Laboratory following the method reported in Ref 19. Our experiments were done using the crystals from the same batch without any special annealing procedure. The chemical composition of one of the crystals was examined with electron probe microanalysis (EPMA) with beam size less than 1 micron. The Lu/Fe ratio was analyzed at 25 randomly selected points on the sample surface. The average Lu/Fe ratio was 1.98 ± 0.02 , and the mean deviation from the average value was less than 1%. This result shows that the Lu and Fe is homogeneously distributed with almost stoichiometric ratio. The oxygen contents of two other pieces were studied using X-ray photoemission spectroscopy (XPS), revealing that the oxygen content in one sample was higher than the other sample, suggesting that there is a small but finite oxygen non-stoichiometry issue in LuFe_2O_4 . It turns out that the magnetic and structural properties of $\text{LuFe}_2\text{O}_{4-\delta}$ depends very sensitively on the oxygen stoichiometry. Detailed study of phase diagram is still in progress, but we made sure that all the samples studied in this work show the same magnetic properties. This ensures that the variation of δ among the samples studied here is very small. The largest piece with a shape of a rectangular parallelepiped ($3 \times 3 \times 1$ mm) was used in our magnetization studies. DC magnetization and AC susceptibility measurements were done using Quantum Design MPMS SQUID magnetometer. Specific heat measurements on the same sample were carried out using thermal relaxation method on Quantum Design PPMS.

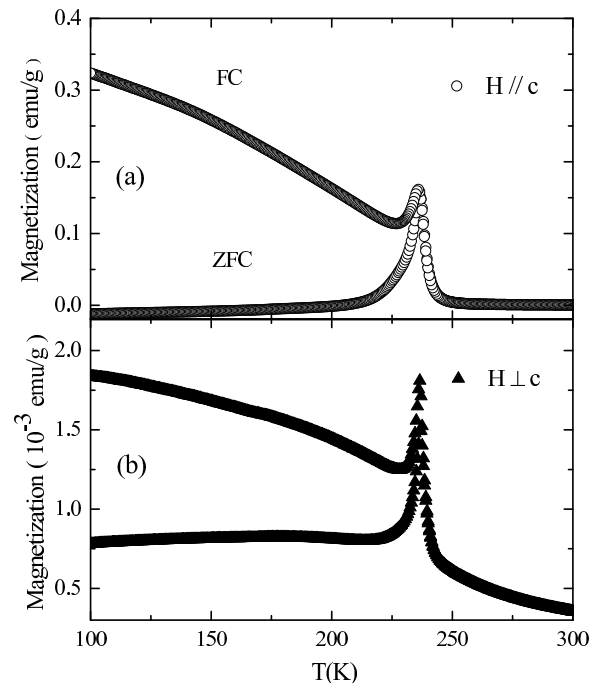


FIG. 1: Temperature dependence of magnetization measured with 10 Oe field applied (a) parallel and (b) perpendicular to the c axis, respectively.

III. EXPERIMENTAL RESULTS

A. DC magnetization

In Fig. 1(a), we show the temperature dependence of the thermo-magnetization of LuFe_2O_4 obtained with 10 Oe field applied parallel to the crystallographic c axis which is perpendicular to the hexagonal planes. A sharp peak appears in the magnetization curve at a temperature of $\sim 236\text{K}$, below which the field-cooled (FC) data begin to diverge from the zero-field-cooled (ZFC) data. In Fig. 1 (b), thermo-magnetization obtained in a field perpendicular to the c axis is shown. Note that the magnetization in this direction is 2 orders of magnitude smaller than that shown in panel (a). This small magnetization can be entirely accounted for by the possible sample misalignment with respect to the field direction. This also illustrates that the easy axis is along the c -axis, and the Ising anisotropy is very large. The non-zero ZFC magnetization at low temperature in this case is probably due to the small residual field in the magnetometer.

B. Specific Heat

Figure 2 shows the temperature dependence of the specific heat, $C(T)$, of the same sample used in the magnetization study. One can identify two features in this curve. The high temperature feature above 300K is rela-

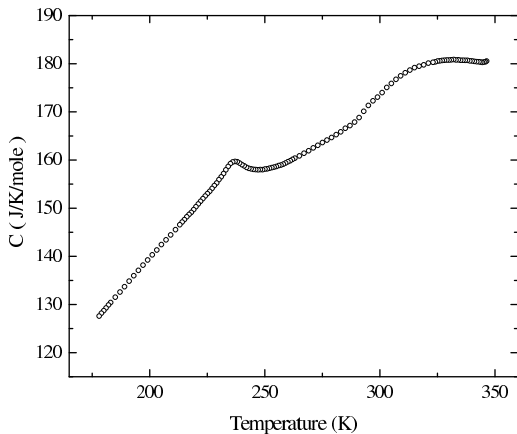


FIG. 2: Temperature dependence of C (T) of sample A measured on continuous cooling.

tively broad and has maximum at ~ 330 K. This feature is probably related to the 3D charge order observed in previous electron and x-ray diffraction studies.⁶ The low temperature peak emerges below ~ 250 K and has a cusp at ~ 237 K. The peak position of this low temperature feature is very close to the peak in magnetic susceptibility, suggesting that this feature is related to the magnetic phase transition.

C. AC susceptibility

Figure 3 shows the real and imaginary part of the AC susceptibility as a function of temperature. The different curves correspond to different driving frequencies of the AC field. The amplitude of AC field was kept constant at $h_{ac}=1$ Oe. A well-defined peak is observed for the real part of the susceptibility χ' at 236 K and the low-temperature tail of this peak decreases with increasing frequency. The imaginary part of the susceptibility, χ'' , appears below ~ 240 K, and consists of two peaks. The high temperature component, appearing as a shoulder, is located at ~ 237 K and grows as frequency increases, while the peak position remains the same. On the other hand, the low temperature peak grows and shifts to higher temperature with increasing frequency. Such a behavior is commonly observed in spin glass systems.

For a spin glass system, with decreasing temperature the spin dynamics become sluggish, so that it takes longer time for a spin to relax, and the maximum relaxation time increases accordingly. When an external AC magnetic field with a driving frequency $\omega/2\pi$ is applied to a spin glass system, if the maximum relaxation time τ_{max} is longer than $\omega/2\pi$, the system will not be able to keep up with the oscillating field and become out of equilibrium. Therefore, one can define the freezing temperature, T_f , as the temperature, at which $\tau_{max} = 2\pi/\omega$. As a result, T_f is a function of driving frequency ω . Experi-

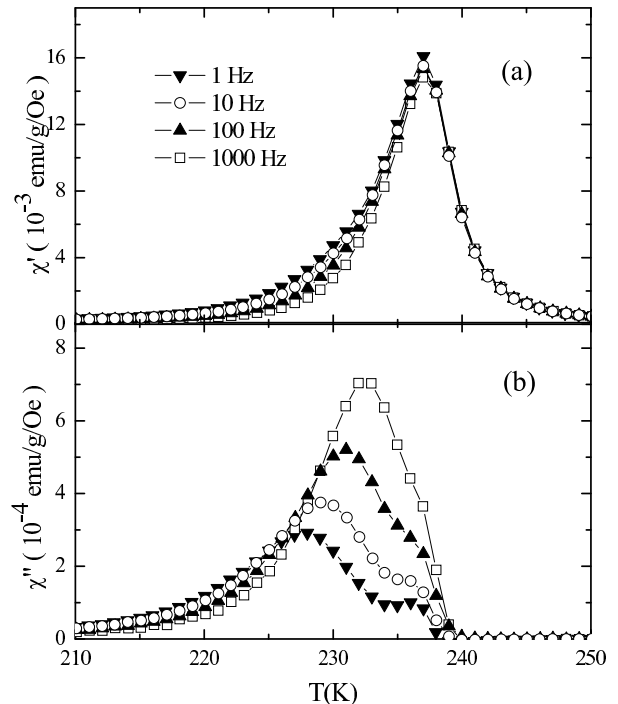


FIG. 3: Temperature dependence of the AC magnetic susceptibility of sample A obtained with different frequencies as labeled. AC field with amplitude $h_{ac}=1$ Oe was applied and the magnetization was measured. The real and imaginary part of the susceptibility are shown in part (a) and (b), respectively.

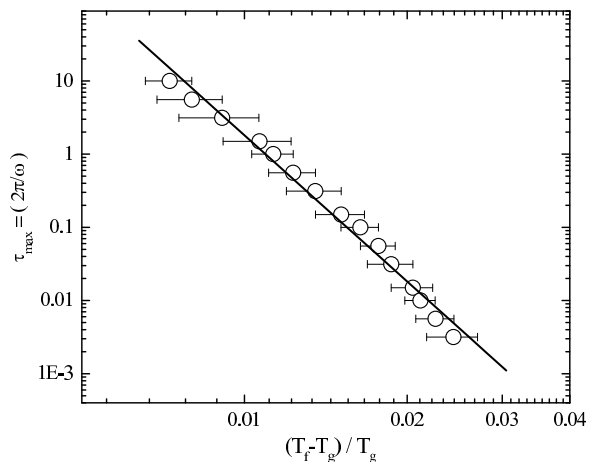


FIG. 4: The dynamic scaling of the reduced temperature vs $\tau_{max}(T_f) = 2\pi/\omega$ in a log-log scale for sample A. The solid line is Eq. 1 with $z\nu = 6.6$, $\tau_0 = 1 \times 10^{-13}$ s and $T_g = 228.5$ K

mentally $T_f(\omega)$ can be determined either from the maximum of $\chi'(\omega)$ or from the inflection point of $\chi''(\omega)$.^{20,21} Since the maximum of χ' is difficult to identify due to the second peak located at 236 K, we use the inflection point of $\chi''(\omega)$ to determine T_f . The maximum relaxation time and $T_f(\omega)$ can be modeled with conventional

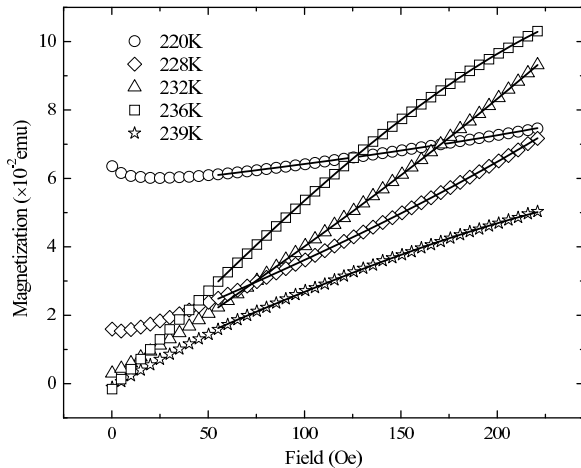


FIG. 5: M vs H curves of LFO at different fixed temperatures measured after cooling under a 200 Oe magnetic field. The solid lines are the fitting results using Eq. 2.

critical slowing down²²

$$\tau_{max} = \tau_0(T_f/T_g - 1)^{-z\nu}, \quad (1)$$

where T_g is the spin-glass transition temperature, z is the dynamical exponent, ν is the usual critical exponent for the correlation length and τ_0 is the microscopic flipping time of the fluctuating spins. The scaling of the AC susceptibility is shown in Fig. 4, and the best fit to Eq. (1) yields $T_g = 228.5 \pm 0.5$ K, $z\nu = 6.6 \pm 1.1$ and $\tau_0 = 10^{-13.0 \pm 1.6}$ s. The value of τ_0 is very close to the microscopic spin flip time $\sim 10^{-13}$ seconds in other spin glass systems.^{21,23} The value of $z\nu$ is within the range of well-known spin-glasses such as CuMn(4.6 at.%) ($z\nu=5.5$)²⁴ and CdCr₂(In)S₄ ($z\nu = 7$).²⁵ This value of $z\nu$ is also close to the value obtained from numerical simulations in three-dimensional (3D) Ising spin glasses.^{26,27,28} This scaling analysis indicates that the low temperature phase is quite possibly a spin-glass phase. Thus, taken together with the heat capacity and the susceptibility data, LFO seems to undergo a continuous phase transition from a Curie paramagnetic phase to ferrimagnetically ordered phase at ~ 236 K and then to a reentrant spin-glass phase below 228K.

D. Nonlinear susceptibility

Figure 5 shows the magnetization (M) versus field (H) curves at different temperatures after cooling under a 200 Oe magnetic field. At low temperatures, since the zero-field magnetization is non-zero, there is thermal remanent magnetization (TRM), which almost vanishes above ~ 232 K. At high temperatures, there is no TRM and the slope of the M vs H curve is largely determined by linear susceptibility, which shows maximum at 236 K (see Fig. 1). At low temperatures, the magnetization initially shows negative slope due to the relaxational behavior of spin-glass phase.

Nonlinear susceptibility is a valuable tool to study the nonlinear behavior of a magnetic phase transition. In particular, the spin-glass susceptibility is believed to be directly proportional to the non-linear susceptibility.^{29,30,31} If a system undergoes a SG phase transition, the magnetization M can be expanded by odd order of H .

$$M = M_0 + a_1H + a_3H^3 + \dots \quad (2)$$

The data in Fig. 5 (above 50 Oe) were fitted using Eq. (2), and the fitting results are shown as solid lines. The constant offset M_0 , linear susceptibility a_1 and the third order nonlinear susceptibility a_3 obtained from the fits are shown in Fig. 6. M_0 starts to grow below ~ 235 K and then increases rapidly below ~ 230 K. The temperature at which M_0 increases rapidly is close to T_g , suggesting that M_0 behaves like the spin-glass order parameter. When the temperature dependence of M_0 below 230K is fitted using $M_0 \sim (T_g - T)^\beta$, best fits are obtained with $T_g = 229$ K and $\beta = 1.0 \pm 0.2$, as shown by the solid line in Fig. 6(a). This critical exponent β is consistent with that of canonical spin-glass systems.^{32,33} The linear susceptibility peak in a_1 at ~ 236 K (Fig. 6(b)) was also observed in DC magnetization and heat capacity, and this indicates the existence of a magnetic phase transition at $T_c \approx 236$ K. If we fit the linear susceptibility for $T > T_c$ to $a_1 \sim (T - T_c)^{-\gamma}$, $\gamma = 1.4 \pm 0.3$ is obtained, and the fitting result is plotted as the solid line in Fig. 6(b). As temperature is lowered, the third order nonlinear susceptibility a_3 shows a negative minimum at 236K, and then it abruptly changes sign at 234K and then show a broad positive peak at ~ 230 K. This behavior is reminiscent of the recent observation that a_3 near a ferromagnetic transition diverges negatively and positively as T_c is approached from above and below, respectively.³⁴ Therefore our observation of the zero-crossing of a_3 around 234K seems to suggest that this high temperature magnetic transition is described as ferrimagnetic (FM) transition. This assignment is also consistent with earlier studies.¹⁶ The behavior of a_3 around 230K, however, is quite unusual for a spin-glass system. It was observed that the nonlinear susceptibility (a_3) is negative with a cusp at the paramagnet to spin glass transition in Ref. 25 and 30. We observe broad positive peak around T_g , which may be due to the reentrant nature of the spin-glass phase in LFO. In fact, similarly unusual behavior have been observed in other reentrant spin-glass systems.^{35,36} Our nonlinear susceptibility data also supports the phase diagram suggested by AC susceptibility data.

E. Non-equilibrium phenomena

Although spins are considered “frozen” in the spin glass phase, due to the slow dynamics, the system simply does not reach the equilibrium state within the experimental time scale. As a result, the spin glass system exhibits non-equilibrium phenomena. One such example

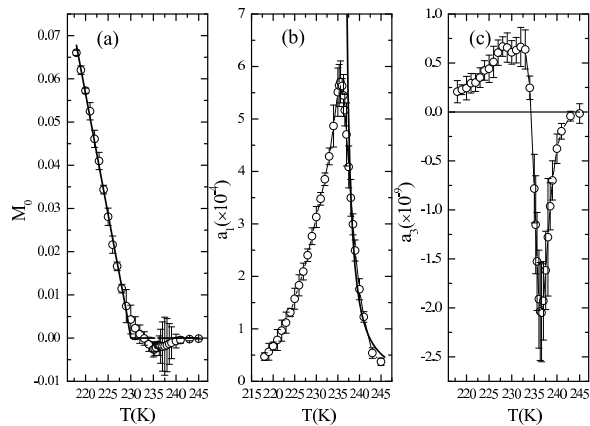


FIG. 6: (a) Constant offset M_0 . The solid line is the fitting using $(T_g - T)^\beta$. (b) Linear susceptibility a_1 . The data above $T_c = 235.6\text{K}$ is fitted by $(T - T_c)^{-\gamma}$, as shown by the solid line. (c) The third order of nonlinear susceptibility a_3 . M_0 , a_1 and a_3 were obtained by fitting the data in Fig. 5 into Eq. 2.

is aging. When a spin-glass system is cooled below T_g , the spin-glass domain grows. Since this domain growth occurs logarithmically in time, it is customary to define the relaxation rate $S \equiv (1/H)\partial M/\partial \log(t)$.³⁷ In Fig. 7, we show our data for $S(t)$ as a function of $\log(t)$. Note that the sample was cooled down to $0.87T_g \sim 200\text{K}$ in the absence of magnetic field. After waiting for a certain time ($t_w=1000\text{s}$, 5000s and 10000s) without external field, the magnetization was recorded as a function of time after a 10 Oe magnetic field was applied. As can be seen from the figure, t at which the maximum relaxation rate occurs increases with increasing t_w , and in fact it is almost equal to t_w . This kind of aging behavior illustrates non-equilibrium dynamics of domain growth, and has been observed in other spin glass systems.^{21,38}

Another interesting example of non-equilibrium dynamics of spin-glass system is the so-called memory effect. In order to show this effect, we have measured temperature dependence of $M(T)$ in two distinct routes. The first, M_{ref} , was obtained by cooling in 10 Oe magnetic field from 300 K down to 50 K at a constant cooling rate of 2 K/min and then heating back continuously at the same rate. In the second route, M was recorded on cooling in 10 Oe at the same rate from 300 K to 50 K with two halts at $T_1 = 160\text{K}$ for 72000 s and at $T_2 = 200\text{K}$ for 48000 s. During the halts, the external field is turned off to let the magnetization relax. After each halt, M shows a clear deviation from the reference as illustrated in Fig. 8, due to aging. After reaching 50 K, the sample temperature is increased continuously at 2 K/min rate in $H = 10\text{Oe}$. During the reheating, the system exhibits a step-like feature at both T_1 and T_2 . The jump at T_1 is not very pronounced, but clear jump in $M(T)$ around T_2 is clearly visible. This suggests that the system somehow remembers the history of halts during cooling. Exceeding

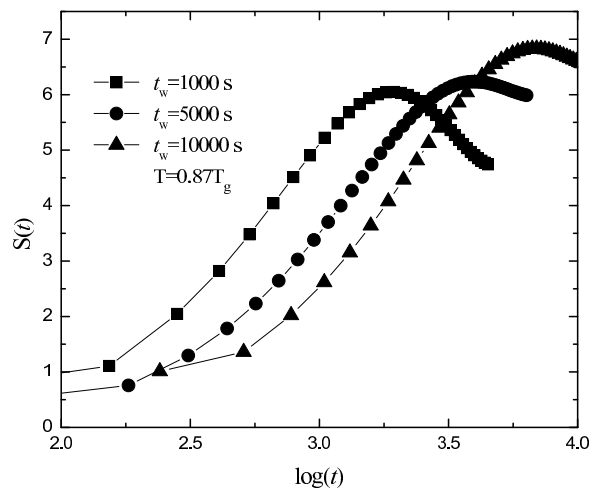


FIG. 7: Relaxation rate S defined in the text is plotted as a function of $\log(t)$ at $T = 0.87T_g$ ($T_g = 228.5\text{K}$). Each curve is obtained by measuring at $H = 10\text{Oe}$ after waiting for t_w following the cool down.

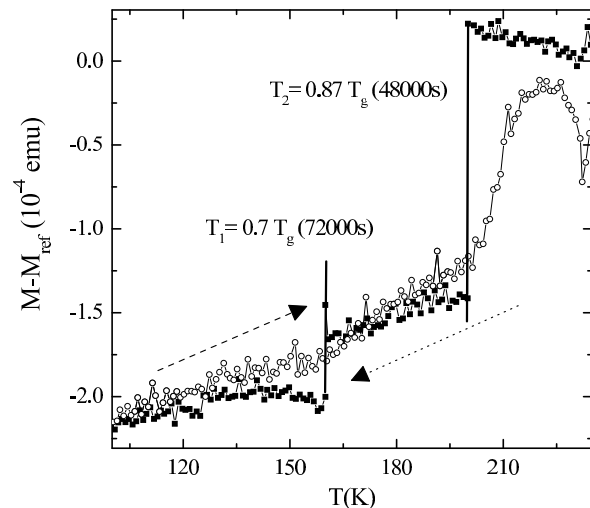


FIG. 8: The relative magnetization $M - M_{ref}$ is plotted as a function of temperature. The magnetization measured on continuous cooling in $H = 10\text{Oe}$ field, is plotted as solid symbols. During the cooling, there were two halts at $T_1 = 0.7T_g$ and $T_2 = 0.87T_g$ ($T_g = 228\text{K}$). The open symbols denote the measurements done on the reheating. The reference M_{ref} was obtained by continuous cooling and reheating in 10 Oe. The cooling and heating rate in both measurements were 2 K/min.

the halt points, M recovers to the reference value and the system is called rejuvenated. Such aging, memory and rejuvenation behavior was observed in other spin glass systems as well.^{23,39,40} These observations also suggest that the low temperature phase of LFO is consistently described as a spin-glass.

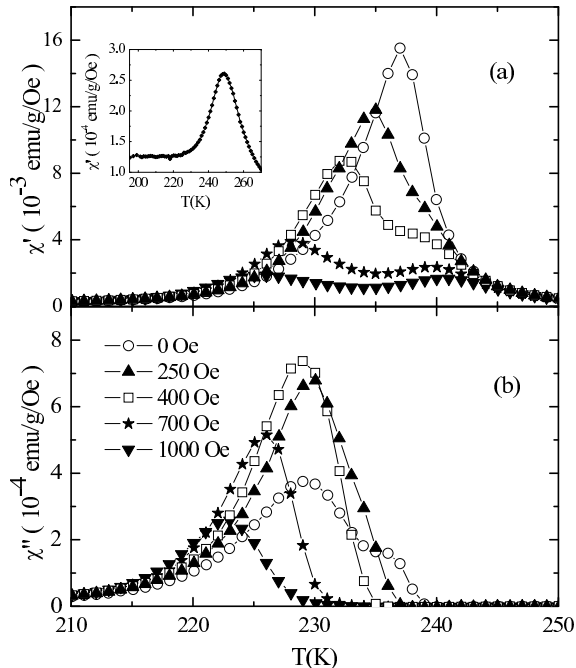


FIG. 9: (a) The real and (b) the imaginary part of AC magnetic susceptibility versus temperature. The driving frequency was fixed at $\omega/2\pi = 10$ Hz and $h_{ac}=1$ Oe. Each curve was obtained under different applied static magnetic field of H . The inset shows the data obtained with $H = 1$ T.

F. Magnetic field dependence

In Fig. 9, AC susceptibility at 10 Hz driving frequency is plotted as a function of temperature for different external static magnetic fields H . As can be seen in the figure, χ' is suppressed by the magnetic field. As the field increases, the main peak of χ' decreases and a double-peak feature emerges. The ferrimagnetic phase transition temperature determined from specific heat and nonlinear susceptibility (~ 236 K) is quite close to the position of the high temperature peak in χ' , which slightly increases with increasing field. The low temperature peaks in χ' and χ'' correspond to the spin-glass transition. As the field increases, the low temperature peak in χ' decreases and finally disappears under ~ 1 T (as shown in the inset). The peak in χ'' also shifts to lower temperature with increasing field. Under very high external field (above 1 T), the spin-glass transition seems to be completely suppressed.

Figure 10 shows the field versus temperature phase diagram. Due to the large uncertainties associated with determining transition temperature of two nearby phase transitions, the error bars at low field is relatively large. However, the field dependence of the PM-FM transition is very weak in this region, while it is clear that the transition temperature gradually increases with increasing field at high field. The spin-glass transition temperature also exhibits substantial field dependence. The SG-FM transition temperature is suppressed rapidly as a small field

is applied. In addition, a threshold field $h_0(\omega) \sim 200$ Oe is observed, below which T_g does not show a systematic change with the change of the field. According to the mean field theory, there exists a phase boundary in $H - T$ phase diagram called de Almeida-Thouless (AT) line,⁴¹ whereby a spin-glass phase can only exist under this boundary (in the low field region). The AT line is given by⁴¹

$$H \propto \left(1 - \frac{T_g(H)}{T_g(0)}\right)^{3/2}, \quad (3)$$

Here H is the external magnetic field and $T_g(H)$ is the field-dependent glass transition temperature.⁴² Our data fits this relation very well as shown in Fig. 10, in which a linear relationship between T_g and $H^{2/3}$ is clearly illustrated.

IV. DISCUSSION

We have presented a variety of experimental evidences showing that the LFO sample goes through re-entrant spin glass transition around 228 K. However, this observation is quite puzzling in several aspects. The first is the microscopic origin of the spin-glass behavior. Conventionally, disordered spin arrangements or interactions (random site or random bond) are necessary to produce magnetic frustration required for spin-glass behavior. However, this system, LFO, is considered highly stoichiometric, and in addition, there exists charge ordering below 300 K, which implies that the arrangement of Fe^{2+} and Fe^{3+} spins are regular. Therefore, this system seems to possess only geometrical frustration as a necessary ingredient for spin glass behavior. Unless spin-glass behavior can arise from pure geometrical frustration, one must find the missing “disorder” in this system to explain the observed spin-glass behavior.

Before discussing the disorder effect in this system, it is useful to examine magnetic interactions present. In LFO, both the Fe^{2+} and Fe^{3+} ions are in their high spin configuration, with the spin angular momentum $S=2$ and $S=5/2$, respectively. The exchange interactions between the Fe^{2+} - Fe^{2+} and Fe^{3+} - Fe^{3+} are presumably antiferromagnetic through the superexchange path via the oxygen ions. However, the magnetic interaction between the Fe^{2+} and Fe^{3+} ions requires further consideration. Note that the Fe^{2+} is in d^6 configuration, and the Hund’s rule dictates that the extra electron in this ion, compared to the Fe^{3+} (d^5) ion should point in the opposite direction of the rest of the “ d^5 ” electrons. Therefore, one can expect the interaction between the Fe^{2+} and Fe^{3+} to be ferromagnetic based on a kinetic energy argument, analogous to the double exchange mechanism in manganites.⁴³ However, since this compound is insulating at all temperatures, such “extra” electron cannot be mobile, but presumably resides in a resonance state between the two neighboring Fe ions.

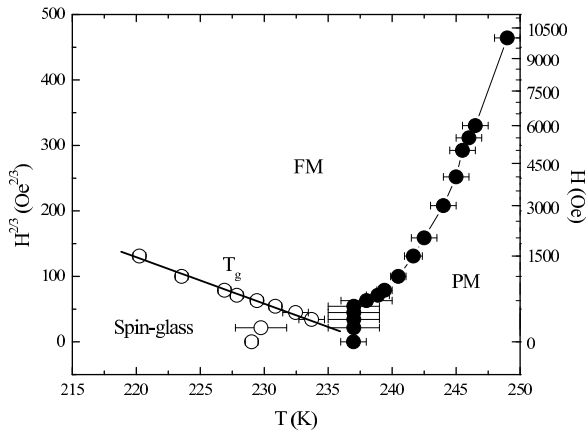


FIG. 10: Field vs. Temperature phase diagram. In order to show AT line, we plot $H^{2/3}$ versus $T_g(\omega)$. The open and closed symbols denote the low and high temperature transition temperatures as described in the text. The thick solid line is the linear fit to the AT line (Eq. 3)

One of the important degrees of freedom in this system, often overlooked, is the orbital degrees of freedom. Since the Fe ions all have trigonal bipyramidal crystal field environment, the 3d orbitals will split into three levels. The highest energy level will be d_{z^2} , and there will be two doubly degenerate orbitals (d_{xy} and $d_{x^2-y^2}$; d_{xz} and d_{yz}) at lower energies. Following the Hund's rule, one can easily see that Fe^{3+} ion has d^5 configuration and is isotropic. However, Fe^{2+} ion has d^6 configuration and the lowest energy orbitals will have orbital degeneracy. In order to break this orbital degeneracy, there could be a cooperative Jahn-Teller distortion of Fe^{2+} ions, once the charge order sets in. Taken together, it is conceivable that two neighboring Fe^{2+} and Fe^{3+} ions form a ‘‘dimer’’, sharing a minority spin electron. In fact, such bond dimerization scenario has been considered in their study of mixed valence B-site Fe ions in Fe_3O_4 by Seo and coworkers.⁴⁴ Such bond dimerization will break the orbital degeneracy, and make the dimer spins form a highly frustrated Kagome lattice, which may be responsible for the observed spin glass behavior. Further structural investigation of this system is required to address this conjecture.

Another important issue is the oxygen non-stoichiometry. If there exists oxygen non-stoichiometry, this will necessarily affect the ratio of Fe^{2+} and Fe^{3+} spins, leading to disorder in charge order, and possibly disorder in the exchange interactions. In fact, our preliminary studies suggest that the oxygen contents seem to change magnetic properties quite dramatically, possibly explaining different magnetic behavior of LuFe_2O_4 compounds reported in the literature.

Another possibility is the charge-ordering model itself. If the charge ordering at 300 K is not of second-order kind, and has some relaxational component, such

as charge glass type ordering, then this will naturally affect the spin ordering part. For example, one can imagine charge-ordered domains exhibiting relaxor type behavior and influence dielectric and magnetic behavior at lower temperatures. Our preliminary x-ray scattering experiments also suggest that the charge ordering in this system is quite complicated and has nontrivial temperature dependence.

Another surprising aspect of the spin-glass transition is its large temperature scale. Almost all known spin-glass systems occur at low temperatures. This is due to the fact that the lower critical dimension of the spin glass transition is believed to be between 2 and 3. Since a 3D SG system is very close to the lower critical dimension, its ordering temperature is very close to absolute zero. In that sense this observation of spin glass behavior at temperatures above 200 K is not only unusual, but very surprising for a quasi 2D system. Again, if the glassy nature of the system arises from the charge sector, this may provide a natural explanation.

V. SUMMARY

The magnetic properties of LuFe_2O_4 single crystals were investigated with DC magnetization and AC susceptibility. Based on the dynamic scaling of AC susceptibility and the behavior of non-linear susceptibility, it is suggested that LuFe_2O_4 goes through first a ferrimagnetic ordering at 236 K, and then subsequently goes through a reentrant spin-glass transition at ~ 228.5 K. Typical properties of spin glass system, such as aging, memory, and rejuvenation have been also observed in this low temperature phase. The field dependence of the spin glass transition temperature is described well by the well-known de Almeida-Thouless theory. It was also observed that the ferrimagnetic transition temperature shows quite sizable field dependence. In order to understand the origin of the spin glass behavior in this compound, possibilities based on the frustration, oxygen non-stoichiometry, and glassy charge ordering have been discussed.

Acknowledgments

We would like to thank David Ellis, S. M. Shapiro, G. Xu, J. Brittain, A. Gershon and H. Zhang for invaluable discussions. The work at University of Toronto was supported by Natural Sciences and Engineering Research Council of Canada, Canadian Foundation for Innovation, Ontario Innovation Trust, and Early Researcher Award by Ontario Ministry of Research and Innovation. The work at Brookhaven was supported by the U. S. Department of Energy, Office of Science.

- * Electronic address: yjkim@physics.utoronto.ca
- ¹ N. Kimizuka, E. Muromachi, and K. Siratori, *Handbook on the Physics and Chemistry of Rare Earths* (Elsevier Science, Amsterdam, 1990), vol. 13, pp. 283–384.
 - ² N. Kimizuka and T. Katsura, *J. Solid State Chem.* **13**, 176 (1975).
 - ³ W. C. Hamilton, *Phys. Rev.* **110**, 1050 (1958).
 - ⁴ J. García and G. Subías, *J. Phys: Condens. Matter* **16**, R145 (2004).
 - ⁵ Y. Tomioka, A. Asamitsu, Y. Moritomo, H. Kuwahara, and Y. Tokura, *Phys. Rev. Lett.* **74**, 5108 (1995).
 - ⁶ Y. Yamada, N. Shinichiro, and N. Ikeda, *J. Phys. Soc. Japan* **66**, 3733 (1997).
 - ⁷ N. Ikeda, H. Ohsumi, K. Ohwada, K. Ishii, T. Inami, K. Kakurai, Y. Murakami, K. Yoshii, S. Mori, Y. Horibe, et al., *Nature* **436**, 1136 (2005).
 - ⁸ Y. Zhang, H. X. Yang, C. Ma, H. F. Tian, and J. Q. Li, *Phys. Rev. Lett.* **98**, 247602 (2007).
 - ⁹ H. J. Xiang and M.-H. Whangbo, *Phys. Rev. Lett.* **98**, 246403 (2007).
 - ¹⁰ M. A. Subramanian, T. He, J. Chen, N. S. Rogado, T. G. Calvarese, and A. W. Sleight, *Adv. Mater.* **18**, 1737 (2006).
 - ¹¹ M. Tanaka, M. Kato, N. Kimizuka, and K. Siratori, *J. Phys. Soc. Japan* **47**, 1737 (1979).
 - ¹² M. Tanaka, J. Akimitsu, Y. Inada, N. Kimizuka, I. Shindo, and N. Siratori, *Solid State Commun.* **44**, 687 (1982).
 - ¹³ Y. Nakagawa, M. Inazumi, N. Kimizuka, and K. Siratori, *J. Phys. Soc. Japan* **47**, 1369 (1979).
 - ¹⁴ N. Ikeda, R. Mori, K. Kohn, M. Mizumaki, and T. Akao, *Ferroelectrics* **272**, 309 (2002).
 - ¹⁵ Y. Nakagawa, M. Kishi, H. Hiroyoshi, N. Kimizuka, and K. Siratori, *Ferrites, Pro. 3rd Int. Conf. Ferrites, Kyoto* (CAPJ, Tokyo, 1981), p. 115.
 - ¹⁶ J. Iida, M. Tanaka, Y. Nakagawa, S. Funahashi, N. Kimizuka, and S. Takekawa, *J. Phys. Soc. Japan* **62**, 1723 (1993).
 - ¹⁷ S. Nagai, M. Matsuda, Y. Ishii, K. Kakurai, H. Kito, N. Ikeda, and Y. Yamada, unpublished.
 - ¹⁸ A. Christianson, M. Lumsden, M. Angst, Z. Yamani, W. Tian, R. Jin, E. Payzant, S. Nagler, B. Sales, and D. Mandrus, arXiv:0711.3560v1.
 - ¹⁹ J. Iida, S. Takekawa, and N. Kimizuka, *J. Cryst Growth* **102**, 398 (1990).
 - ²⁰ J. Mattsson, T. Jonsson, P. Nordblad, H. ArugaKatori, and A. Ito, *Phys. Rev. Lett.* **74**, 4305 (1995).
 - ²¹ K. Gunnarsson, P. Svedlindh, J. O. Andersson, P. Nordblad, L. Lundgren, H. ArugaKatori, and A. Ito, *Phys. Rev. B* **46**, 8227 (1992).
 - ²² P. C. Hohenberg and B. I. Halperin, *Rev. Mod. Phys.* **49**, 435 (1977).
 - ²³ R. Mathieu, D. Akahoshi, A. Asamitsu, Y. Tomioka, and Y. Tokura, *Phys. Rev. Lett.* **93**, 227202 (2004).
 - ²⁴ J. A. Mydosh, *Spin Glass: An Experimental Introduction* (Taylor & Francis, London, 1993).
 - ²⁵ E. Vincent and J. Hammann, *J. Phys. C* **20**, 2659 (1987).
 - ²⁶ I. A. Campbell, *Phys. Rev. B* **37**, 9800 (1988).
 - ²⁷ A. T. Ogielski, *Phys. Rev. B* **32**, 7384 (1985).
 - ²⁸ A. T. Ogielski and I. Morgenstern, *Phys. Rev. Lett.* **54**, 928 (1985).
 - ²⁹ A. P. Ramirez, G. P. Espinosa, and A. S. Cooper, *Phys. Rev. Lett.* **64**, 2070 (1990).
 - ³⁰ M. J. P. Gingras, C. V. Stager, B. D. Gaulin, N. P. Raju, and J. E. Greedan, *J. Appl. Phys.* **79**, 6170 (1996).
 - ³¹ F. Rivadulla, M. A. López-Quintela, and J. Rivas, *Phys. Rev. Lett.* **93**, 167206 (2004).
 - ³² H. Bouchiat, *J. Phys. (Paris)* **47**, 71 (1986).
 - ³³ S. Wakimoto, S. Ueki, Y. Endoh, and K. Yamada, *Phys. Rev. B* **62**, 3547 (2000).
 - ³⁴ S. Nair and A. Banerjee, *Phys. Rev. B* **68**, 094408 (2003).
 - ³⁵ I. S. Suzuki and M. Suzuki, *Phys. Rev. B* **73**, 94448 (2006).
 - ³⁶ T. Sato, T. Ando, T. Ogawa, S. Morimoto, and A. Ito, *Phys. Rev. B* **64**, 184432 (2001).
 - ³⁷ K. H. Fischer and J. A. Hertz, *Spin glasses* (Cambridge University Press, Cambridge, UK, 1991).
 - ³⁸ L. Lundgren, P. Nordblad, P. Svedlindh, and O. Beckman, *J. Appl. Phys.* **57**, 3371 (1985).
 - ³⁹ E. Vincent, V. Dupuis, M. Alba, J. Hammann, and J. P. Bouchaud, *Europhys. Lett.* **50**, 674 (2000).
 - ⁴⁰ K. Jonason, E. Vincent, J. Hammann, J. P. Bouchaud, and P. Nordblad, *Phys. Rev. Lett.* **81**, 3243 (1998).
 - ⁴¹ J. R. L. de Almeida and D. J. Thouless, *J. Phys. A* **11**, 983 (1978).
 - ⁴² H. A. Katori and A. Ito, *J. Phys. Soc. Japan* **63**, 3122 (1994).
 - ⁴³ C. Zener, *Phys. Rev.* **82**, 403 (1951).
 - ⁴⁴ H. Seo, M. Ogata, and H. Fukuyama, *Phys. Rev. B* **65**, 85107 (2002).